Testing QED Screening and Two-Loop Contributions with He-Like Ions

H. Bruhns,* J. Braun, K. Kubiček, J. R. Crespo López-Urrutia, and J. Ullrich

Max-Planck-Institut für Kernphysik, 69117 Heidelberg, Germany

(Received 9 May 2007; published 11 September 2007)

We report wavelength measurements of H-like and He-like ions obtained with a novel x-ray spectrometer at the Heidelberg Electron Beam Ion Trap. The experimental uncertainty for the Lyman-α_1 wavelength in Cl^{16+} is reduced by a factor of 3 and, as expected, excellent agreement with theory is maintained. For the resonance line in He-like Ar^{16+}, an uncertainty of only $\delta\lambda/\lambda = 2 \times 10^{-6}$ was achieved. This is the most precise x-ray wavelength reported for highly charged ions to date, and allows to test recent predictions on QED two-electron and two-photon radiative corrections for He-like ions. The results also point to the advantages of establishing absolute x-ray wavelength standards using Lyman-α transitions (in the present case Ar^{17+} Lyman-α_1) to supersede the current ones.

DOI: 10.1103/PhysRevLett.99.113001 PACS numbers: 32.30.Rj, 31.10.+z, 31.25.Eb, 31.30.Jv

The $1S$-$2S$ transition wavelength in hydrogen, recently measured to $\delta\lambda/\lambda = 2 \times 10^{-14}$ by the group of Hänsch [1], constitutes an experimental cornerstone of atomic theory and quantum electrodynamics (QED), which, with quantum field theories in general, are the foundations of our current understanding of particle interactions. The present experimental precision exceeds by far that of predictions, especially since the proton radius affecting them is not known accurately enough. The laboratory result can thus be used for predicting other transitions in hydrogen to achieve relative theoretical uncertainties smaller than that of the Rydberg constant [2].

Going further, the scaling of the strength of the nuclear Coulomb field by orders of magnitude in highly charged ions (HCI) allows testing QED in its nonperturbative limit since the electronic binding energy to a nucleus with charge Z renders the $(Z\alpha)$-perturbation expansion (α is the fine structure constant), well suited to low-Z systems, not applicable anymore. Newly developed all-order nonperturbative calculations [3] agree with measurements in HCI, even in the extreme case of H-like uranium U^{91+} [4]. Here, with QED and nuclear size contributions scaling up with Z^4 to nearly 500 eV, predictions accurate on the level of 0.5 eV still exceed the experimental precision by a factor of 10.

At the same time, the theory of few-electron ions isoelectronic to helium and lithium has been refined. Difficulties arise here from the evaluation of the interelectronic correlation. For He-like ions, the unified method (UM) of Drake [5] employs accurate correlated two-electron nonrelativistic wave functions perturbatively corrected for QED and relativistic effects. In contrast, the all-order (AO) method of Plante [6] uses a fully relativistic two-body, i.e., one-electron, calculation adding QED and electronic interaction with the Breit approximation. A similar approach has been applied in a very recent calculation by Artemyev *et al.* [7]. It is important to note that AO calculations apply the QED corrections calculated within the UM, while Artemyev *et al.* provide a new, *ab initio* QED prediction within an all-order approach dubbed here bound-state QED (BSQED). Disregarding QED corrections for the moment, the UM is expected to be more accurate at low Z since correlation effects are more relevant than relativistic ones, whereas the AO and BSQED methods should perform better at high Z, where relativistic effects become dominant. Around $Z \approx 26$, both relativistic and correlation effects are of comparable size. Thus, over a wide range of "medium" Z, accurate accounting of all relativistic, correlation, and QED effects is required.

On the experimental side, several measurements of the $1s2p\,{}^1P_1 \rightarrow 1s^2\,{}^1S_0$ resonance transition (abbreviated "w" [8]) in He-like ions ranging from S ($Z = 16$) [9] to Kr ($Z = 36$) [10] have been reported. The most accurate one ($\Delta\lambda/\lambda = 12$ ppm) was performed for Ar^{16+} ($Z = 18$) by Deslattes *et al.* [11]. Even this (for HCI small) uncertainty did not allow, by a factor of 5, to distinguish among the various predictions.

The present experiment at the Heidelberg Electron Beam Ion Trap (HD-EBIT) aims at solving this situation. One of the most serious problems here is the quality of present x-ray wavelength standards. The most accurate ones ($K\alpha$ lines excited in metals [12]) display skewed line shapes due to multiple excitations inducing unresolvable satellite transitions. Finding the line centroid with high precision is practically impossible. In contrast to this, Lyman-α transitions in H-like ions trapped in an EBIT do not suffer from this problem (Fig. 1) and can be used as reference based on the 1 ppm precision claimed by theory. This seems well justified for medium-Z ions, but it has not been confirmed experimentally. Using theoretical Lyman-α wavelengths as references for the He-like transitions of the same element gives a major advantage: The BSQED calculations start from uncorrelated one-electron wave functions (corresponding to a H-like ion) and then introduce two-electron effects as corrections. Hence, one can subtract all two-electron contributions (with the sole exception of the nuclear recoil correction) and arrive at the value of Lyman-α_1. Discrepancies between experiment

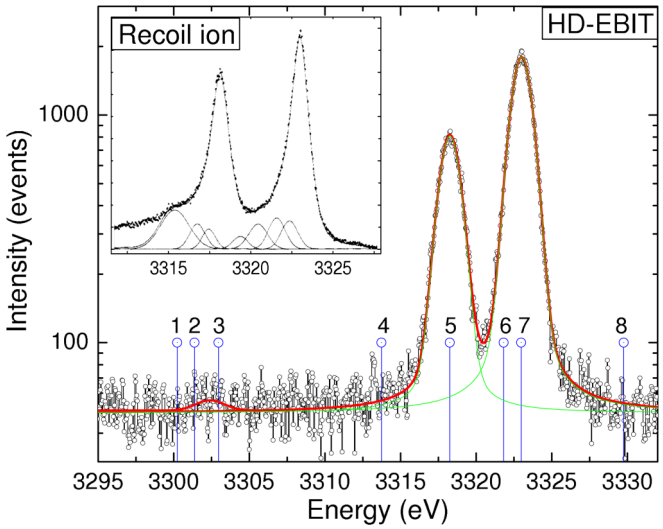

FIG. 1 (color online). Observed Lyman-α_1 (7) and Lyman-α_2 (5) lines in Ar^{17+} (HD-EBIT), Voigt fit and predicted [25] satellites on a logarithmic scale. Only satellite 6 has a possible contribution estimated through a Gaussian fitted to the data near satellite 2. This one shares a common $2s2p\,^1P_1$ upper level but has a much higher transition probability than the other. The inferred maximum intensity contribution of satellite 6 to Lyman-α_1 line is 2.5×10^{-5}, i.e., insignificant. Insert: Lyman-α spectrum of Ar^{17+} (linear scale) obtained with the recoil ion method [22], the previously most precise measurement of x-ray transitions in HCI. Dots: experiment; full curve: fit using arbitrary satellite components.

and theory can thus be assigned to the two-electron corrections. Indeed, the energy predicted by BSQED for He-like Ar with all two-electron contributions subtracted is in good agreement with the Lyman-α_1 energy calculated by Johnson and Soff [13] for H-like ions.

The experiment was performed using the HD-EBIT (see, e.g., [14]) with an electron beam current of 400 mA at about 10 keV kinetic energy to produce and trap the H-like and He-like ions in a cylindrical volume of ≈ 100 μm diameter and 4 cm length. A novel x-ray spectrometer allows to alternately observe the Lyman-α_1 wavelength transition in Ar^{17+} and the other transitions of interest, often several hundred eV away, while keeping the same angular calibration. A partial description of the setup, an analysis of its error sources and long time stability, are found in [15]. That instrument has been upgraded [16] to apply the so-called "Bond method" (see, e.g., Hölzer *et al.* [12]) for absolute wavelength measurements.

The experimental procedure basically consists of rotating a flat [here Si (111)] crystal reflecting x rays at a Bragg angle Θ_B towards either one of two symmetrically arranged, windowless, cryogenically cooled CCD detectors. A rotation by $180° - 2\Theta_B$ results in a reflection of the x rays towards the other detector. From the measured angular difference, the exact Bragg angle Θ_B can be determined without uncertainties resulting from an offset of the angular scale. To assure that the pathway of the reflected x rays from the source (EBIT) to the crystal is exactly the same for both crystal orientations, a new method was developed to eliminate the otherwise necessary collimating apertures and the resulting intensity losses. We introduced two laser beams originating from a virtual source overlapping with the trapped ions. These beams are specularly reflected at the polished crystal surface towards any of the CCD cameras. Their observed positions there are used as fiducials. The ratio of the distances of the x-ray line on the CCD to the two fiducials yields the necessary information about the actual pathway of the reflected x-ray beam from the trapped ions to the position on the crystal surface at which it fulfills Bragg's condition. The geometry of the three beams (lasers, x-ray) originating from a common source is very convenient since due to the theorem of intersecting lines, the distance ratios at the detector are insensitive to the unavoidable mechanical displacements of camera and crystal and only depend on the actual crystal angle. For the alignment of the laser fiducials, two retractable lenses collect visible light emitted by trapped B-like Ar^{13+} ions and image them (after a reflection on the crystal surface) onto the CCD detectors to ensure perfect overlap of the adjustable virtual source and the ions. The EBIT and the spectrometer were computer controlled, thus keeping the temperature-stabilized laboratory undisturbed for several days during runs in which up to a few hundred spectra of the references and lines of interest were recorded alternately. As seen in Fig. 1, the resolution is better than FWHM < 1.8 eV at 3323 eV. After various modifications, sources of uncertainty related to stability and alignment have been significantly reduced in comparison with our earlier proof-of-principle work [15]. The angle ϕ between the crystal surface and the Si (111) plane was carefully measured, yielding $\phi = 0.0585° \pm 0.002°$. The orientation of the Si (111) plane with respect to the crystal shape is also known with a precision of $\pm 2°$. The crystal is mounted on a holder that can be rotated around the surface normal axis to set the orientation of ϕ to be perpendicular to the scattering plane in such a way that it does not affect the measured difference angle. At the accuracy given for this rotation adjustment, we estimate the remaining contribution to the total uncertainty to be 0.5 ppm [16]. Another small contribution to the overall uncertainty is variations of the lattice spacing due to temperature.

Apart from counting statistics, the remaining leading uncertainty for these *absolute* measurements arises from the minute curvature of the lines on the CCD detector. X rays emitted by the ions trapped at the EBIT, an extended line source, project after Bragg reflection a series of circular segments (or, more generally, conical sections) on the CCD cameras. Consequently, when adding up the CCD pixel signals along the nondispersive detector axis to obtain spectra, the resulting line profiles are intrinsically

asymmetric. This cannot directly be observed because symmetric line broadening effects (thermal, crystal defects) dominate the line shape, but the asymmetric profile shifts the line centroid to higher energies on the level of 40 ppm. This (calculable) shift is partially compensated (here: by ≈ 15 ppm) if the line source center lies outside the scattering plane because this results both in a change of the effective crystal lattice spacing and of the line curvature shift described above. Unfortunately, a final uncertainty of the *absolute* wavelength measurements of roughly 20 ppm cannot be excluded. However, this figure can be significantly reduced in a *relative* wavelength measurement using a known reference wavelength. Indeed, the effect of all these systematic contributions can be comprised in a correction angle $\Delta\Theta_{\mathrm{corr}}$ later to be added to the absolutely measured Bragg angle Θ_a of the line of interest. To determine $\Delta\Theta_{\mathrm{corr}}$, we calculate the predicted Ar^{17+} Lyman-α_1 Bragg angle Θ_t

$$\Theta_t = \arcsin\left[\frac{1}{4d}(\lambda_t + \sqrt{\lambda_t^2 + 16d^2\delta_\lambda})\right] \qquad (1)$$

from the theoretical wavelength λ_t [13] using the refractive index of the Si (111) crystal δ_λ and its lattice constant d, and subtract it from the measured absolute Lyman-α_1 Bragg angle. As the correction angle $\Delta\Theta_{\mathrm{corr}}$ depends on the Bragg angle, it was scaled from Θ_t to Θ_a using a scaling factor obtained from a ray-tracing simulation [16] of the x-ray trajectories. Using this procedure, the results shown with 1σ error bars in Table I for Lyman-α_1 transition in Cl^{16+} and for w in Ar^{16+} were obtained in wavelength units (m) and converted to energy using $hc = 1.239841875(31) \times 10^{-6}$ eV m [17]. To our knowledge, the present results are the most accurate of any x-ray transition in HCI to date and, therefore, can be used to test the theory of two-electron ions most stringently. All earlier reported experimental Cl Lyman-α_1 transition wavelengths [18–20] have to be corrected to the latest available [21] recommended wavelength values of their Ar $K\alpha$ reference lines. None of those measurements had an uncertainty smaller than 100 meV. Our result with an error bar of only 30 meV is the only one sensitive to test the vacuum polarization contribution of 68 meV [18].

We want to emphasize the value for the Ar^{16+} w transition, for which we have the most extensive data sets. The result, $\lambda_w = 3949.066(8)$ mÅ, or $E_w = 3139.583(6)$ eV, has an error of only 2 ppm, a factor of 3 smaller than our preliminary value [15], a factor of 6 better than the most precise measurement in any He-like ion [11], and 2.5 times more accurate than any x-ray wavelength in HCI thus far reported. The theoretical Lyman-α_1 wavelength was chosen as reference because its uncertainty is much smaller than the 5 ppm (17 meV) of the experimental data of Beyer [22], who used $K\alpha$ standard lines of K in crystalline KCl for calibration.

This result is in excellent agreement with BSQED [7] and AO predictions within its 2 ppm uncertainty. The UM prediction lies just on the edge of our 1σ error estimate. This rather small discrepancy could arise from an incomplete description of relativistic effects at $Z = 18$ in UM. However, replacing the UM's own QED corrections with the more recent ones of BSQED (see Table II) shifts UM values by 10 meV to higher energies, bringing UM to agree with BSQED within 1.5 ppm despite its supposedly incomplete relativistic treatment. If the same is done for AO, where the UM's QED corrections were used, the previously perfect agreement between AO and BSQED (as well as with our experimental result) worsens. Hence, the BSQED's QED corrections seem better than those of UM, and the BSQED electron correlation treatment proves to be more complete than that of AO. As shown in Table II, our result is sensitive to all two-electron QED contributions to the $^1S_0$ ground state energy, i.e., screened self-energy, screened vacuum polarization, and two-photon exchange diagrams as calculated in [7] at a level of 6% of their total. Also, the total one-electron QED correction of the $^1P_0$ excited state is probed, but the accuracy is too low to test the 3 meV two-electron contribution. However, two-loop corrections to the ground state due to exchange of two virtual photons (9 meV) are a factor of 1.5 larger than the present uncertainty. Table III displays the results for the different QED terms obtained in the BSQED and UM calculations.

In Fig. 2, we compare the present results for the w line with other previous theoretical and experimental work in He-like ions. Although we now establish excellent agreement with the predictions of BSQED [7], and good with [5,6] at $Z = 18$, a rigorous test will still require extending these measurements over a broader range of elements.

In summary, absolute wavelength measurements in x-ray lines free from satellite contributions emitted by H-like Cl^{16+} and He-like Ar^{16+} ions were corrected for a small, not yet fully quantified systematic shift due to the line

TABLE I. Present experimental results compared with theory.

Transition	E_{theor} (eV)	E_{expt} (eV)	Error (ppm)
Cl^{16+} Ly-α_1	2962.352 [13]	2962.344(30)	10
Ar^{16+} w	3139.582 [7]	3139.583(6)	1.9

TABLE II. Theoretical one- and two-electron QED contributions in the $1s2p\ ^1P_1$ and $1s^2\ ^1S_0$ states in the Ar^{16+} ion (from [7]) in eV. Total 1-el.: sum of one-electron contributions; Scr. SE: screened self-energy; Scr. VP: screened vacuum polarization; 2-ph. exch.: exchange of two virtual photons; total 2-el.: sum of two-electron contributions. Not listed are total higher-order contributions of less than 1 meV.

State	Total 1-el.	Scr. SE	Scr. VP	2-ph. exch.	Total 2-el.
$^1S_0$	−1.1310	0.1116	−0.0072	−0.0091	0.0953
$^1P_1$	−0.0062	0.0031	−0.0001	0.0001	0.0031

TABLE III. Comparison between BSQED [7] and UM [5] predictions for the upper and lower states of the Ar^{16+} $1s2p\,^1P_1 \rightarrow 1s^2\,^1S_0$ (w) transition. BSQED: E_{Dirac}: one-electron Dirac value; E_{int}: electron-electron interaction correction; E_{QED}: total QED correction; E_{rec}: relativistic recoil correction. UM: $E_{\text{non-rel}}$: nonrelativistic two-electron ground state energy; E_{rel}: relativistic corrections; E_{QED}: QED correction; E_{nucl}: sum of mass polarization and finite nuclear size correction.

	BSQED [7] level energy contributions [eV]					UM [5] level energy contributions [eV]				
State	E_{Dirac}	E_{int}	E_{QED}	E_{rec}	E_{sum}	$E_{\text{non-rel}}$	E_{rel}	E_{QED}	E_{nucl}	E_{sum}
$^1S_0$	4427.4154	−305.6560	−1.0366	−0.0575	4120.6653	4106.337	15.377	−1.046	−0.009	4120.659
$^1P_1$	1103.2520	−118.6220	−0.0032	−0.0162	981.0832[a]	978.996	2.099	−0.004	−0.008	981.083

[a]Contributions from quasidegeneracy with $^3P_1$ not listed.

curvature by using the theoretical value of the (at present level of accuracy well understood) Ar^{17+} Lyman-α_1 transition, thus effectively referencing them to theory of the H-like system. The result obtained for the $1s2p\,^1P_1 \rightarrow 1s^2\,^1S_0$ resonance transition (w line) in He-like Ar^{16+} has an uncertainty of only 2 ppm, and, being the most precise reported in HCI to date, becomes sensitive to binding energy QED contributions at the level of two-electron screening and two-photon diagrams. The Lyman-α_1 transition energy in H-like Cl is also about a factor of 3 more precise than in any previous experiment. Work in progress to further reduce uncertainties down to the 1 ppm level could allow testing higher-order contributions as well. The spectral purity of satellite-free lines produced by H-like ions in EBITs clearly suggests to use Lyman-α wavelengths as high-precision, absolute and calculable atomic x-ray standards, which are also needed for future synchrotron and free-electron laser resonance fluorescence studies

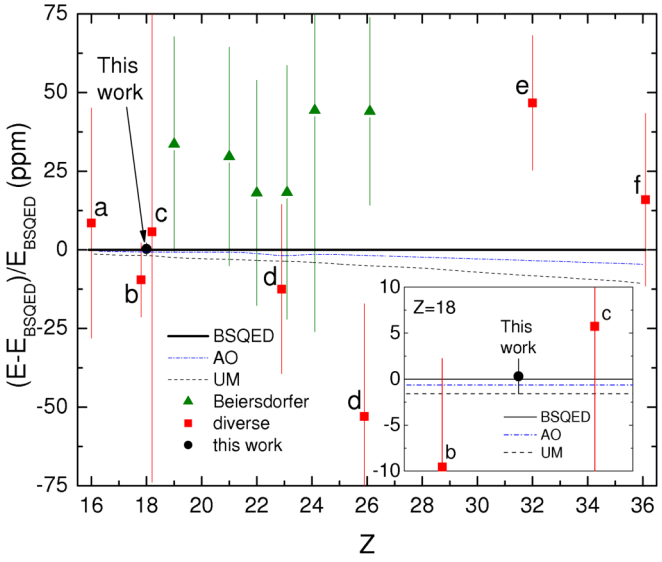

FIG. 2 (color online). Comparison of experimental data for the $1s2p\,^1P_1 \rightarrow 1s^2\,^1S_0$ (w) transition energy with theory. UM: unified method [5]; AO: all-order [6]; BSQED: bound-state QED [7]. Experimental data taken from Beiersdorfer: [26], (a): [9], (b): [11], (c): [27], (d): [28], (e): [29], (f): [10]. The insert magnifies $Z = 18$.

[23] as well as for the characterization of x-ray microcalorimeters currently being developed in several laboratories [24] for astrophysical and other spectroscopic applications.

We would like to thank Professor E. Förster for scientific discussions and the characterization of our crystal and also acknowledge helpful discussions with Z. Harman.

*Present address: Columbia Astrophysics Laboratory, Columbia University, NY, NY 10027-6601, USA
hbruhns@astro.columbia.edu

[1] M. Niering *et al.*, Phys. Rev. Lett. **84**, 5496 (2000).
[2] U. D. Jentschura *et al.*, Phys. Rev. Lett. **95**, 163003 (2005).
[3] V. A. Yerokhin and V. M. Shabaev, Phys. Rev. A **64**, 062507 (2001).
[4] A. Gumberidze *et al.*, Phys. Rev. Lett. **94**, 223001 (2005).
[5] G. W. F. Drake, Can. J. Phys. **66**, 586 (1988).
[6] D. R. Plante *et al.*, Phys. Rev. A **49**, 3519 (1994).
[7] A. N. Artemyev *et al.*, Phys. Rev. A **71**, 062104 (2005).
[8] A. H. Gabriel, Mon. Not. R. Astron. Soc. **160**, 99 (1972).
[9] L. Schleinkofer *et al.*, Phys. Scr. **25**, 917 (1982).
[10] K. Widmann *et al.*, Phys. Rev. A **53**, 2200 (1996).
[11] R. D. Deslattes *et al.*, J. Phys. B **17**, L689 (1984).
[12] G. Hölzer *et al.*, Phys. Rev. A **56**, 4554 (1997).
[13] W. R. Johnson and G. Soff, At. Data Nucl. Data Tables **33**, 405 (1985).
[14] A. Lapierre *et al.*, Phys. Rev. A **73**, 052507 (2006).
[15] J. Braun *et al.*, Rev. Sci. Instrum. **76**, 073105 (2005).
[16] J. Braun, Ph.D. thesis, Max-Planck-Institut für Kernphysik, Heidelberg, 2006.
[17] P. J. Mohr *et al.*, http://physics.nist.gov/constants.
[18] E. Källne *et al.*, J. Phys. B **17**, L115 (1984).
[19] P. Richard *et al.*, Phys. Rev. A **29**, 2939 (1984).
[20] R. D. Deslattes *et al.*, Phys. Rev. A **32**, 1911 (1985).
[21] R. D. Deslattes *et al.*, Rev. Mod. Phys. **75**, 35 (2003).
[22] H. F. Beyer *et al.*, J. Phys. B **18**, 207 (1985).
[23] S. W. Epp *et al.*, Phys. Rev. Lett. **98**, 183001 (2007).
[24] F. S. Porter *et al.*, Rev. Sci. Instrum. **75**, 3772 (2004).
[25] L. A. Vainshtein, At. Data Nucl. Data Tables **21**, 49 (1978).
[26] P. Beiersdorfer *et al.*, Phys. Rev. A **40**, 150 (1989).
[27] J. P. Briand *et al.*, Phys. Rev. A **28**, 1413 (1983).
[28] C. T. Chantler *et al.*, Phys. Rev. A **62**, 042501 (2000).
[29] S. MacLaren *et al.*, Phys. Rev. A **45**, 329 (1992).